American Mineralogist, Volume 76, pages 1449–1454, 1991

Shear and volume relaxation in $Na_2Si_2O_5$

SHARON L. WEBB
Bayerisches Geoinstitut, Universität Bayreuth, Postfach 101251, Bayreuth, Germany

ABSTRACT

The relaxed and unrelaxed shear and volume moduli of $Na_2Si_2O_5$ have been determined over a temperature range of 950–1200 °C and frequency range of 5–150 MHz using ultrasonic techniques. The relaxed volume modulus ($K_0 \cong 20$ GPa) and the unrelaxed volume modulus ($K_\infty \cong 25$ GPa) of the melt have been calculated from the combination of the longitudinal moduli ($M_0 \cong 20$ GPa; $M_\infty \cong 39$ GPa) and shear moduli ($G_0 = 0$ GPa; $G_\infty = 10$ GPa). The ~19 GPa increase in longitudinal modulus is made up of both a shear contribution (13 GPa) and a volume contribution (5 GPa) resulting from the loss of both the shear and volume relaxation processes with increasing frequency of the applied sinusoidal stress.

INTRODUCTION

The rheology of magmas is of fundamental importance in understanding the occurrence of igneous rocks, the buoyant rise or fall of magma bodies, and the behavior of melts at high pressures (Agee and Walker, 1988; Rigden et al., 1989; Harris et al., 1970). Melt rheology can be determined from both stress-strain rate (viscosity) and stress-strain (modulus) measurements. Three linear regimes of strain occur in a stressed melt. These are (1) instantaneous recoverable elastic deformation, (2) delayed recoverable anelastic deformation, and (3) delayed nonrecoverable viscous deformation (Nowick and Berry, 1972). It is the time scale ($2\pi \cdot$frequency = time scale^{-1}) of observation of the melt behavior that determines whether elastic, anelastic, viscous, or viscoelastic rheology is observed. (Viscoelastic rheology is the sum of the elastic, anelastic, and viscous responses.) If it were possible to measure the deformation of a melt instantaneously upon application of a stress, only the elastic component of the deformation would be observed, and the unrelaxed Newtonian glass rheology of the melt would be determined. When the shear deformation of a melt is observed a long time after the application of a stress (for melts of viscosity 10^{-2}–10^5 Pa s, a long time scale is greater than 1 ns–10 ms; see Eq. 1), only delayed viscous deformation takes place, and relaxed, Newtonian, viscous liquid rheology is observed. In the case of volumetric deformation, silicate melts behave as anelastic materials and no delayed viscous flow is observed. Both the instantaneous and the long time scale observation of melt deformation result in the determination of Newtonian (i.e., strain-rate independent) rheology. However, if the deformation of the melt is observed on a time scale similar to the time scale on which the delayed, recoverable deformation takes place, non-Newtonian time-dependent (strain-rate dependent) linear viscoelastic rheology of the melt will be observed.

The change in melt rheology from elastic to viscoelastic is due to the relaxation of the structure of the melt. In the case of a simple melt with one structural relaxation process and one relaxation time, the Maxwell relationship defines the relaxation time τ;

$$\tau = \frac{\eta}{\mathcal{M}_\infty} \quad (1)$$

where η is the (long time scale) Newtonian viscosity and $\mathcal{M}_\infty$ is the elastic (infinite frequency) modulus of the melt. This relationship applies for both volume (η_v, K_∞) and shear (η_s, G_∞) deformation (Gruber and Litovitz, 1964). The relaxation time τ can be recast in terms of a relaxation strain rate $\dot{\gamma}$ and a relaxation frequency Ω ($\Omega = 2\pi f_\tau$), where $\tau^{-1} = \dot{\gamma} = \Omega$. Therefore, with increasing strain rate (or decreasing time scale of observation or increasing frequency of applied signal), non-Newtonian (or time-dependent or frequency-dependent) behavior is expected. In cases where the stress-strain rate relationship has been investigated over a significant range of strain rate, both Newtonian (Scarfe et al., 1983) and non-Newtonian (pseudoplastic) behavior (Li and Uhlmann, 1970; Webb and Dingwell, 1990) have been observed in silicate melts.

The relaxation time curve for any melt composition can be plotted (from Eq. 1) as a function of inverse temperature, given the temperature dependence of the shear viscosity and assuming the shear modulus to be a constant. {Given the relative temperature invariance of G_∞ [$\log_{10} G_\infty$ (Pa s) = 10 ± 0.5] with respect to the order-of-magnitude changes in viscosity associated with changes in temperature, it is reasonable to set G_∞ to 10 GPa (Dingwell and Webb, 1989).} Figure 1 illustrates that it is possible to cross from relaxed to unrelaxed melt rheology by holding the time scale of observation constant and varying the temperature at which the melt properties are observed (A′-B′). In the present determination of melt rheology, the temperature of the melt is held constant and the time scale (frequency^{-1}) of observation changed (A-B). For a melt of shear viscosity 10^3 Pa s and shear mod-

0003–004X/91/0910–1449$02.00

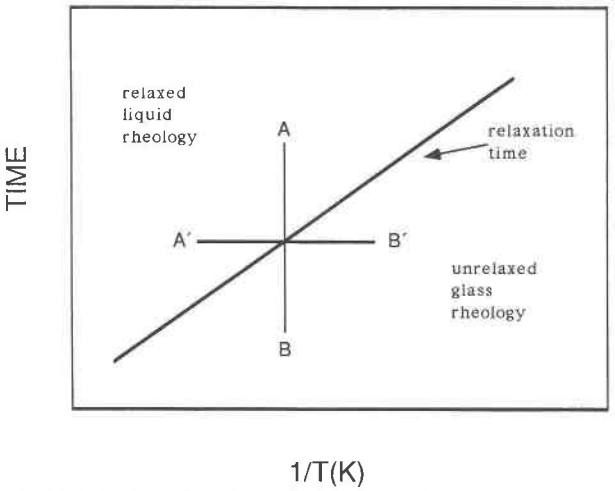

Fig. 1. Relaxation time as a function of inverse temperature. It is possible to cross from relaxed to unrelaxed rheology by holding the observation time constant and varying the temperature along A′-B′ or by holding the temperature constant and varying the observation time along A-B.

ulus of 10 GPa, the relaxation time $\tau \simeq 100$ ns [$\dot{\gamma} \simeq 10^7$ s^{-1}, $\Omega \simeq 10$ MHz ($f_r = 1.6$ MHz)]. It is therefore difficult to perform measurements in the time domain on a time scale shorter than this relaxation time. High frequency ultrasonics or Brillouin scattering techniques can, however, be used to measure the relaxed (liquid) and unrelaxed (glass) rheology of silicate melts and to observe the frequency dependence of both viscosity and modulus in the vicinity of the relaxation frequency. Given that the strain resulting from the application of a stress is time dependent, the modulus and viscosity observed are also time dependent, with modulus increasing with frequency (decreasing with time) and viscosity decreasing with frequency (increasing with time) (Dingwell and Webb, 1989).

The Maxwell relationship has been employed in ultrasonic studies of longitudinal relaxation in silicate melts (e.g., Manghnani et al., 1981; Sato and Manghnani, 1985; Rivers and Carmichael, 1987) to describe the distribution and temperature dependence of the longitudinal relaxation time (combining the high frequency longitudinal modulus and the Newtonian shear viscosity in Eq. 1). [Note that the factor of 0.01 is required to fit the Maxwell equation to Rivers and Carmichael's data because the zero frequency shear viscosity data reported in their Table 5 is 2 orders of magnitude larger than those in the original references (Dingwell and Webb, 1989).] The interpretation of such measurements is difficult because the longitudinal relaxation process is a mixture of both volume and shear processes. Assuming single relaxation times for both shear (τ_s) and volume (τ_v) processes, the frequency-dependent shear modulus can be described by

$$G^*(\omega) = \frac{G_\infty \omega^2 \tau_s^2}{1 + \omega^2 \tau_s^2} + i \frac{G_\infty \omega \tau_s}{1 + \omega^2 \tau_s^2} \quad (2)$$

where $\omega = 2\pi f$ and G_∞ is the elastic (infinite frequency) shear modulus; the frequency-dependent volume (bulk) modulus is

$$K^*(\omega) = K_0 + \frac{K_1 \omega^2 \tau_v^2}{1 + \omega^2 \tau_v^2} + i \frac{K_1 \omega \tau_v}{1 + \omega^2 \tau_v^2} \quad (3)$$

where the elastic (infinite frequency) volume modulus $K_\infty = K_0 + K_1$ (Herzfeld and Litovitz, 1959). The longitudinal modulus $M^*(\omega)$ is

$$M^*(\omega) = K^*(\omega) + 4G^*(\omega)/3. \quad (4)$$

Therefore, at frequencies much lower than the relaxation frequency, relaxed (liquid) frequency-independent behavior is expected for the volume, longitudinal, and shear moduli, with the shear modulus being zero and $K^*(\omega) = M^*(\omega)$. At frequencies much greater than the relaxation frequency, unrelaxed (glass) frequency-independent moduli are again expected, with the shear modulus being nonzero and $K^*(\omega) < M^*(\omega)$. For frequencies in the vicinity of the relaxation frequency, frequency-dependent (non-Newtonian) behavior is expected, with the modulus (and therefore the velocity) increasing with increasing frequency. The volume and shear viscosities of the melt can also be calculated from the moduli as (Litovitz and Davis, 1965)

$$\eta^*(\omega) = \frac{\mathcal{M}^*(\omega)}{i\omega} = \frac{\mathcal{M}'(\omega) + i\mathcal{M}''(\omega)}{i\omega}$$
$$= \frac{\mathcal{M}''(\omega) - i\mathcal{M}'(\omega)}{\omega} \quad (5)$$

for modulus $\mathcal{M}$.

Most ultrasonic studies of silicate melts are conducted at the high-temperature (1000–1500 °C) and low-frequency (3–22 MHz) conditions required to observe the relaxed (frequency-independent) longitudinal modulus of the melt. In cases where the experimental conditions were approaching the relaxation frequency of the melt [e.g., Manghnani et al., 1981 (basalt melts); Sato and Manghnani, 1985 (basalt melts); Rivers and Carmichael, 1987 (silicate melts)], frequency dependence of the longitudinal modulus has been observed. In studies where the frequency of the applied signal has been greater than that of the relaxation frequency of the melt, shear wave propagation has been observed [Tauke et al., 1968 (B_2O_3); Macedo et al., 1968 (Na_2O-B_2O_3-SiO_2)].

In the present study, the viscosity (10^1–10^3 Pa s) and frequency (5–150 MHz) ranges were chosen such that both relaxed and unrelaxed shear and longitudinal moduli and viscosities could be determined, with the volume modulus being calculated from Equation 4.

Experimental technique

The $Na_2Si_2O_5$ glass was prepared from reagent-grade Na_2CO_3 and SiO_2 powders that were dried at 400 °C overnight. Fifty grams of the powder mix was fused in a $Pt_{95}Au_5$ crucible at 1200 °C until bubble free. The composition of the glass at the end of the measurements is listed in Table 1. The gradual loss of Na during the ultrasonic measure-

TABLE 1. Microprobe analysis of $Na_2Si_2O_5$ glass

Weight percent	
SiO_2	65.92
Fe_2O_3	0.04
MoO_2	0.02
Na_2O	32.44
Total	98.42

Note: Cameca SX-50 wavelength dispersive analysis using 15 kV, 15 nA on brass, 30-μm defocused beam, 20-s count times. Standard: synthetic glass DGG1.

ments results in the viscosity of the melt increasing to 0.05 $\log_{10}$ units more than that of $Na_2Si_2O_5$ (Lillie, 1939).

The velocity and attenuation of both shear and longitudinal waves were determined at ultrasonic frequencies (5–150 MHz) using a furnace and twin buffer-rod setup similar to that of Macedo and Litovitz (1965). The furnace is a Mo wound-tube furnace. The buffer rods are single crystals of Mo 210 mm long and 12 mm in diameter, aligned along the [100] axis. There was a constant flow of forming gas (95%N_2-5%H_2) across both the furnace elements and the Mo buffer rods. Five-MHz chrome-gold coaxially plated quartz AC-cut shear and X-cut compressional wave transducers were used at frequencies tween the first and 15th harmonic. The cylindrical surfaces of both buffer rods and crucible have grooves 0.5 mm deep in order to reduce the side-wall reflections of the ultrasonic waves. As there are two buffer rods in this system, a compressional wave transducer is glued (using Crystal Bond) to the lower rod and a shear wave transducer to the upper rod. The measurements are performed in the reflection mode, with each transducer acting as both sender and receiver.

The interferometric technique of Katahara et al. (1981) was used. The buffer rods were aligned at room temperature at 145 MHz in acetone using the compressional wave signal. Pulsed sinusoidal signals of 40 μs duration were propagated through the melt, and the change in amplitude of the returned signal (the sum of a semi-infinite number of echoes within the melt) was monitored as the

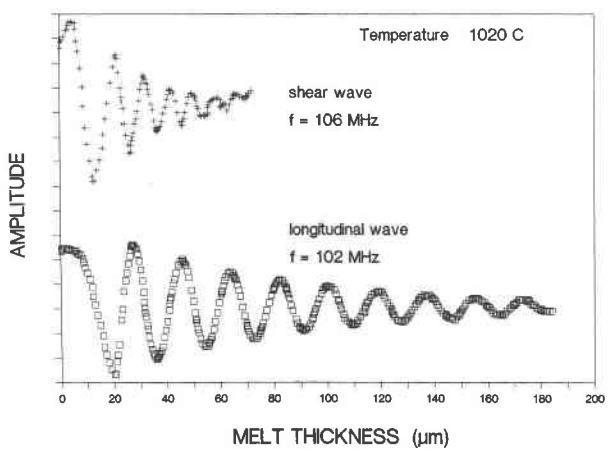

Fig. 2. Shear and longitudinal wave interference patterns at 106 and 102 MHz, respectively, and 1020 °C.

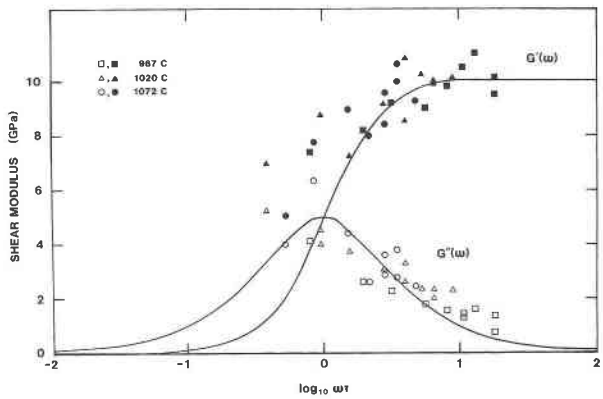

Fig. 3. The frequency-dependent shear modulus $G^*(\omega) = G'(\omega) + iG''(\omega)$ as a function of normalized angular frequency. The shear relaxation time for each temperature is calculated from Equation 1 with $G_\infty = 10$ GPa. The estimated error in the measured moduli is less than 5%. The curve is calculated from Equation 2.

upper buffer rod was moved. The amplitude of the reflected signal is

$$|A_r|^2 = \frac{R^2[\exp(4\alpha L) - 2\exp(2\alpha L)\cos(4\pi Lf/c) + 1]}{\exp(4\alpha L) - 2R^2\exp(2\alpha L)\cos(4\pi Lf/c) + R^4} \quad (6)$$

(Rivers, 1985) where α is the attenuation coefficient, L the melt thickness, c the signal velocity, and R is the reflection coefficient at the buffer rod-melt interface, where

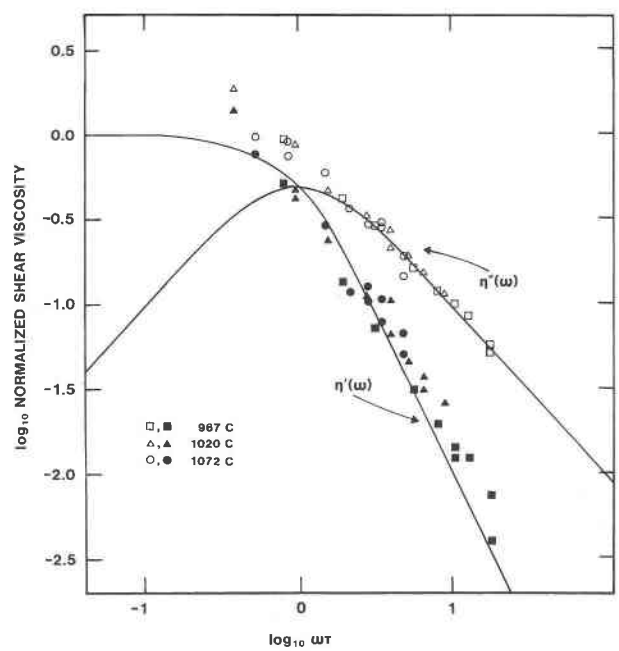

Fig. 4. The frequency-dependent shear viscosity $\eta^*(\omega) = \eta'(\omega) + i\eta''(\omega)$ as a function of normalized frequency. The shear viscosity is also normalized to the Newtonian viscosity of the melt. The curve is calculated from Equation 5. The $\log_{10}$ of the absolute value of the imaginary viscosity term is plotted.

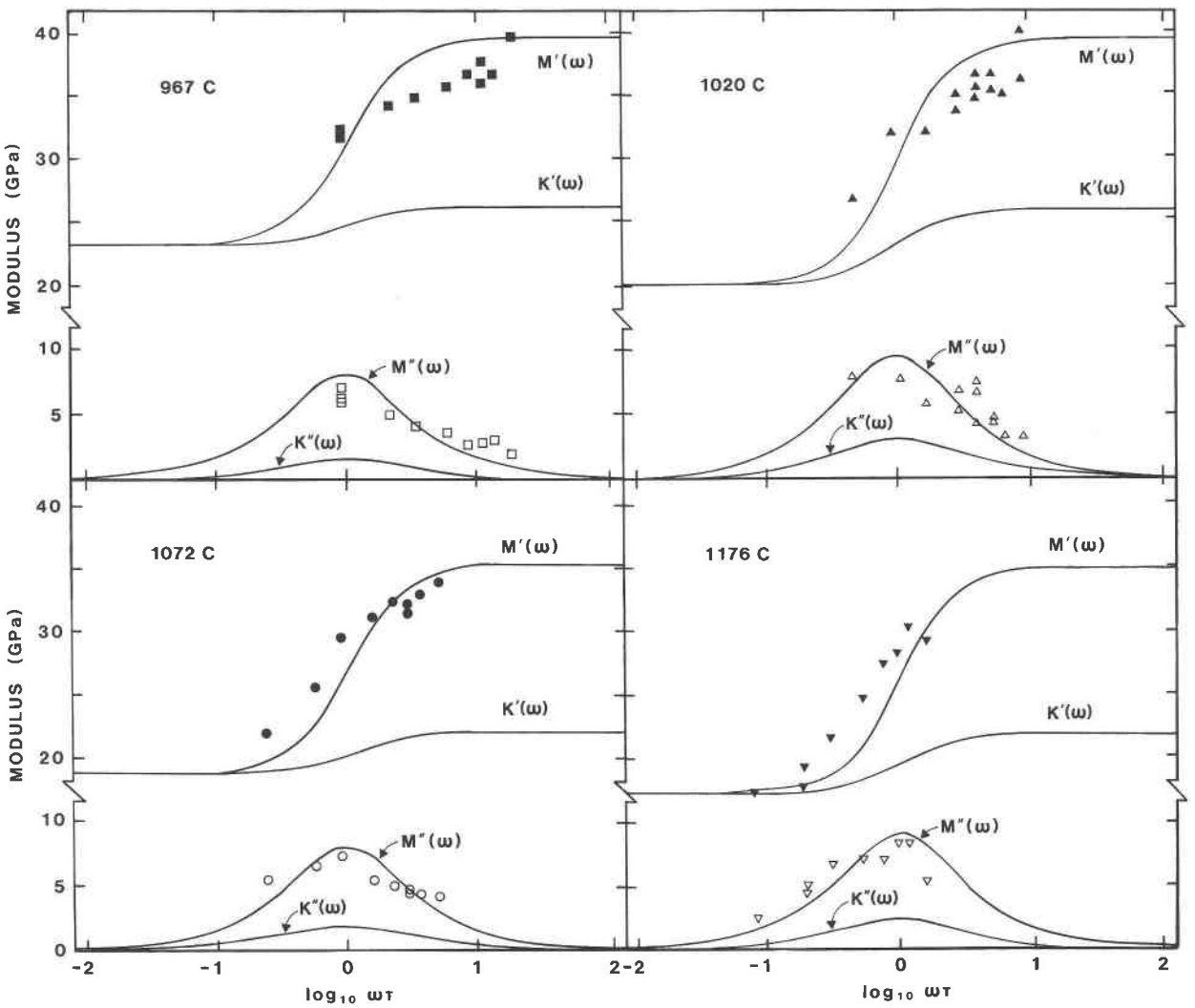

Fig. 5. The frequency-dependent longitudinal $M^*(\omega) = M'(\omega) + iM''(\omega)$ and volume $K^*(\omega) = K'(\omega) + iK''(\omega)$ moduli as a function of temperature and normalized frequency. The estimated errors in the measured moduli are less than 5%. The curves are calculated from Equations 2 and 3.

$$R = \frac{\rho_{melt}c_{melt} - \rho_{Mo}c_{Mo}}{\rho_{melt}c_{melt} + \rho_{Mo}c_{Mo}} \quad (7)$$

and ρ and c are density and velocity for the melt and Mo. The density of the Mo buffer rods was taken to be 10.213 g/cm³ (Bujard, 1982), and the high-temperature velocities of shear and compressional waves traveling through Mo along [100] were taken from Bujard (1982). The density of the melt was calculated from Stein et al. (1986).

Results and discussion

Figure 2 illustrates the signal amplitude vs. melt thickness data obtained from both shear and longitudinal wave propagation at 106 and 102 MHz, respectively, and 1020 °C shear viscosity 10^2 Pa s (Fontana and Plummer, 1979). The amplitude vs. thickness data were fit to Equation 6, resulting in the calculation of velocity and attenuation. The real component of the modulus $\mathcal{M}'(\omega) = \rho c^2$ and the imaginary component of the modulus $\mathcal{M}''(\omega) = \mathcal{M}'(\omega)c\alpha/\pi f$ [where the quality factor $Q = \mathcal{M}'(\omega)/\mathcal{M}''(\omega) = \pi f/c\alpha$; O'Connell and Budiansky, 1978] were then calculated for each temperature and frequency condition.

The frequency dependence of the real and imaginary components of the shear modulus and shear viscosity of $Na_2Si_2O_5$ are illustrated in Figures 3 and 4, respectively. The curves drawn in Figures 3 and 4 are those for Equation 2, where the relaxation time τ_s has been calculated as $\tau_s = \eta/G_\infty$. Frequency has been normalized using the relaxation time at each temperature. No shear mode propagation was observed at 1176 °C. The frequency-independent unrelaxed shear modulus was found to be 10.0 ± 0.3 GPa and independent of temperature in the range 967–1072 °C. This unrelaxed shear modulus is slightly lower than that determined by Mills (1974) (13.7 GPa) using torsion techniques in the temperature range 414–512 °C. A value for dG_∞/dT of −0.007 GPa/°C is

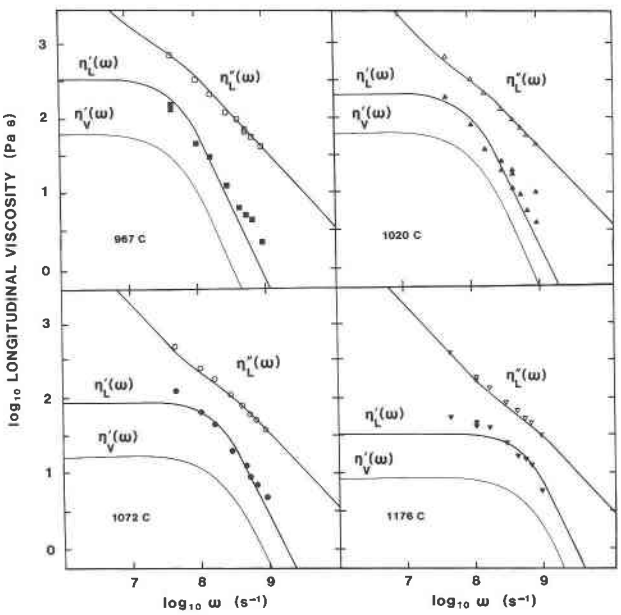

Fig. 6. The frequency-dependent longitudinal $\eta_L^*(\omega) = \eta_L'(\omega) + i\eta_L''(\omega)$ and volume $\eta_v'(\omega)$ viscosity as a function of normalized frequency. The $\log_{10}$ of the absolute value of the imaginary viscosity term is plotted. There is no appreciable difference between $\eta_L''(\omega)$ and $\eta_v''(\omega)$. The curves are calculated from Equation 5.

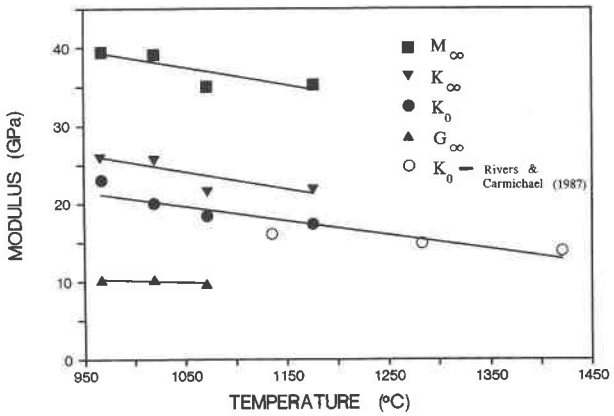

Fig. 7. The temperature dependence of the unrelaxed shear (G_∞) and longitudinal (M_∞) moduli and the relaxed (K_0) and unrelaxed (K_∞) volume moduli. The open symbols are the data of Rivers and Carmichael (1987). The lines are fits to the data.

required to reconcile these high- and low-temperature determinations of the infinite frequency shear modulus. This is somewhat smaller than the value $dG_\infty/dT = -0.025$ GPa/°C observed by Macedo et al. (1968) in an alkali-borosilicate melt in the viscosity range $10^{1.7} < \eta < 10^{4.2}$ Pa s.

The viscosity data in Figure 4 have been normalized to the Newtonian shear viscosity of the melt at each temperature. At low frequencies, where the relaxed liquid properties of the melt are observed, the frequency-dependent viscosity approaches the Newtonian viscosity determined by concentric cylinder techniques.

The frequency dependence of the real and imaginary parts of the longitudinal and volume moduli and viscosities of $Na_2Si_2O_5$ are illustrated in Figures 5 and 6. It was not possible with the limited low-frequency data to determine the volume relaxation time. Tauke et al. (1968) calculated the shear and volume relaxation times in liquid B_2O_3 and found that $0.8\tau_s \leq \tau_v \leq \tau_s$. Therefore, the shear relaxation time τ_s was used in the present study to fit Equations 4 and 5 to the longitudinal data. The paucity of low-frequency data for both longitudinal and shear wave propagation also resulted in inability to calculate any distribution in τ_s in time space. Any distribution in τ_s will result in the broadening of the frequency range over which the real and imaginary parts of the modulus and viscosity are frequency dependent. If $\tau_v \cong \tau_s$, a similar broadening will occur for the longitudinal modulus. (In the extreme case that there is more than an order of magnitude difference between τ_v and τ_s, two separate peaks will be observed in the imaginary component of the longitudinal modulus, and two frequency-dependent regimes will be observed in the real component of the modulus.)

The low-frequency volume and longitudinal moduli are identical [$G^*(\omega) = 0$ for $\omega \ll \tau^{-1}$] and approximately 20 GPa. With increasing frequency, as the melt structure can no longer relax on the time scale of the applied sinusoidal stress, the longitudinal modulus increases to ~39 GPa. However, 13 GPa of this increase is due to the propagation of a high frequency shear wave through the unrelaxed melt. The unrelaxed volume modulus of the melt is therefore ~25 GPa, an increase of 5 GPa from the relaxed value. The temperature dependence of the relaxed and unrelaxed longitudinal, volume, and shear moduli of $Na_2Si_2O_5$ are illustrated in Figure 7 (see Table

TABLE 2. The relaxed and unrelaxed moduli and viscosities of $Na_2Si_2O_5$

T	M_∞	K_∞	K_0	K_1	G_∞	η_v'	η_s	ρ
°C			GPa			$\log_{10}$(Pa s)		g/cm³
967	39.51	26.18	23.07	3.11	10.12	1.80	2.31	2.296
1020	39.14	25.81	20.12	5.69	10.16	1.76	2.00	2.285
1072	35.07	21.74	18.56	3.18	9.71	1.24	1.74	2.273
1176	35.36	22.03	17.40	4.63		0.92	1.29	2.251

Note: M_∞ = unrelaxed longitudinal modulus; K_∞ = unrelaxed volume modulus; G_∞ = unrelaxed shear modulus; K_0 = relaxed volume modulus; η_s = relaxed shear viscosity; η_v' = relaxed volume viscosity. The shear viscosities are from Fontana and Plummer (1979), and the densities are calculated from Stein et al. (1986).

2). Included in Figure 7 are the high-temperature ultrasonic data of Rivers and Carmichael (1987).

Conclusion

The theory of relaxation in melts as discussed by Herzfeld and Litovitz (1959) predicts that shear waves will propagate through a silicate melt when the frequency of the wave is greater than the relaxation frequency of the melt. In the present study it has been shown that the unrelaxed shear modulus of $Na_2Si_2O_5$ is 10 GPa and that the observed increase in longitudinal modulus from ~20 GPa to ~39 GPa in going from liquid to glass rheology is mainly due to the unrelaxed shear modulus, with the unrelaxed volume modulus being only ~5 GPa greater than the relaxed volume modulus.

Acknowledgments

Kurt Klasinski is thanked for interfacing all of the electronics and programming the data acquisition system. The program to fit the data was developed by C. Ross II. The starting glass was provided by D.B. Dingwell. The microprobe analysis was performed by D. Krauße.

References cited

Agee, C.A., and Walker, D. (1988) Static compression and olivine flotation in ultrabasic silicate liquid. Journal of Geophysical Research, 93, 3437–3449.

Bujard, P. (1982) Comportement élastique singulier d'alliages de métaux de transition paramagnétiques VB-VIB, 195 p. Thesis, Université de Genéve, Geneva, Switzerland.

Dingwell, D.B., and Webb S.L. (1989) Structural relaxation in silicate melts and non-Newtonian melt rheology in geologic processes. Physics and Chemistry of Minerals, 16, 508–516.

Fontana, E.H., and Plummer, W.A. (1979) A viscosity-temperature relation for glass. Journal of the American Ceramic Society, 62, 367–369.

Gruber, G.J., and Litovitz, T.A. (1964) Shear and structural relaxation in zinc chloride. Journal of Chemical Physics, 40, 13–26.

Harris, P.G., Kennedy, W.Q., and Scarfe, C.M. (1970) Volcanism versus plutonism: The effect of chemical composition. Geological Journal, Special Issue No. 2, 187–200.

Herzfeld, K.F., and Litovitz, T.A. (1959) Absorption and dispersion of ultrasonic waves, 535 p. Academic Press, New York.

Katahara, K.W., Rai, C.S., Manghnani, M.H., and Balogh, J. (1981) An interferometric technique for measuring velocity and attenuation in molten rocks. Journal of Geophysical Research, 86, 11779–11786.

Li, J.H., and Uhlmann, D.R. (1970) The flow of glass at high stress levels. Journal of Non-Crystalline Solids, 33, 235–248.

Lillie, H.R. (1939) High-temperature viscosities of soda-silica glasses. Journal of the American Ceramic Society, 22, 367–374.

Litovitz, T.A., and Davis, C.A. (1965) Structural and shear relaxation in liquids. In W.P. Mason, Ed., Physical acoustics, vol. 2A, p. 281–349. Academic Press, New York.

Macedo, P.B., and Litovitz, T.A., (1965) Ultrasonic viscous relaxation in molten boron trioxide. Physics and Chemistry of Glasses, 6, 69–80.

Macedo, P.B., Simmons J.H., and Haller, W. (1968) Spectrum of relaxation times and fluctuation theory: Ultrasonic studies on an alkali-borosilicate melt. Physics and Chemistry of Glasses, 9, 156–164.

Manghnani, M.H., Rai, C.S., Katahara, K.W., and Olhoeft, G.R. (1981) Ultrasonic velocity and attenuation in basalt melt. Anelasticity in the Earth, vol. 4, p. 118–122. American Geophysical Union, Washington, DC.

Mills, J.J. (1974) Low frequency storage and loss moduli of soda silica glasses in the transformation range. Journal of Non-Crystalline Solids, 14, 255–268.

Nowick A.S., and Berry, B.S. (1972) Anelastic relaxation in crystalline solids, p. 677. Academic Press, New York.

O'Connell, R.J., and Budiansky, B. (1978) Measures of dissipation in viscoelastic media. Geophysical Research Letters, 5, 5–8.

Rigden, S.M., Ahrens, T.J., and Stolper, E.M. (1989) High-pressure equation of state of molten anorthite and diopside. Journal of Geophysical Research, 94, 9508–9522.

Rivers, M.L. (1985) Ultrasonic studies of silicate melts, 215 p. Ph.D. thesis, University of California, Berkeley, California.

Rivers, M.L., and Carmichael, I.S.E. (1987) Ultrasonic studies of silicate melts. Journal of Geophysical Research, 92, 9247–9270.

Sato, H., and Manghnani, M.H. (1985) Ultrasonic measurements of V_p and Q_p: Relaxation spectrum of complex modulus of basalt melts. Physics of the Earth and Planetary Interiors, 41, 18–33.

Scarfe, C.M., Cronin, D.J., Wenzel, J.T., and Kaufman, D.A. (1983) Viscosity-temperature relationship at 1 atm in the system diopside-anorthite. American Mineralogist, 68, 1083–1088.

Stein, D.J., Stebbins, J.F., and Carmichael, I.S.E. (1986) Density of molten sodium aluminosilicates. Journal of the American Ceramic Society, 69, 396–399.

Tauke, J., Litovitz, T.A., and Macedo, P.B. (1968) Viscous relaxation and non-Arrhenius behavior in B_2O_3. Journal of the American Ceramic Society, 51, 158–163.

Webb, S.L., and Dingwell, D.B. (1990) The onset of non-Newtonian rheology of silicate melts. Physics and Chemistry of Minerals, 17, 125–132.

Manuscript received July 9, 1990
Manuscript accepted May 17, 1991